LANGMUIR Article
Cite This: Langmuir 2019, 35, 7155−7160
pubs.acs.org/Langmuir

Enhancing Printing Resolution on Hydrophobic Polymer Surfaces Using Patterned Coatings of Cellulose Nanocrystals

Ragesh Prathapan,[†] Bernhard Alexander Glatz,[‡,§] Anik Kumar Ghosh,[‡] Stefan Michel,[‡] Andreas Fery,[‡,∥] Gil Garnier,[⊥] and Rico F. Tabor*[,†]

[†]School of Chemistry and [⊥]Bioresources Processing Research Institute of Australia (BioPRIA), Department of Chemical Engineering, Monash University, Clayton, VIC 3800, Australia

[‡]Institute of Physical Chemistry and Polymer Physics, Leibniz Institute of Polymer Research, 01069 Dresden, Germany

[§]University of Bayreuth Graduate School, University of Bayreuth, Universitätsstr. 30, 95477 Bayreuth, Germany

[∥]Physical Chemistry of Polymeric Materials, Technical University Dresden. Mommsenstr. 4, 01062 Dresden, Germany

Supporting Information

ABSTRACT: High-resolution inkjet printing of a hydrophobic polymer surface (polystyrene, PS) was accomplished using a patterned coating of cellulose nanocrystals (CNCs) that prevents the ink from bleeding. A periodically crack-free, wrinkled (wavelength of around 850 nm) stamp was prepared by surface oxidation of an uniaxially stretched poly(dimethylsiloxane) elastomeric substrate and was used as a template to transfer aligned patterns of cellulose nanocrystals (CNCs) onto PS surfaces by wet stamping. The morphology of the aligned CNC coatings on PS was then compared with randomly deposited CNCs on PS using atomic force microscopy. The wettability of the CNCs and polymer surfaces with water and ink was measured and analyzed in the context of inkjet printing. This biomaterial coating technique enables high-resolution printing of modern water-based inks onto hydrophobic surfaces for applications in renewable packaging and printing of biomolecules for high throughput diagnostics. Further, with suitable modifications, the technology is scalable to roll-to-roll manufacturing for industrial flexo printing.

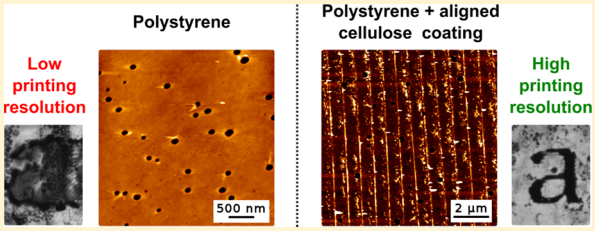

1. INTRODUCTION

Selective printing on various polymers using inkjet technology is central to a range of applications including drug delivery devices, fabrication of full color polymer displays, transistors, and biodiagnostics.[1−5] The stability of the ink, its spreading and adhesion to the surface, as well as substrate roughness and chemical composition all contribute to the quality and resolution of printing.[6] Significant effort has been devoted to modifying inks for this purpose—mainly by tailoring their composition and rheology or incorporating functional additives such as metallic particles. Park et al.[7] investigated inkjet printing (piezoelectric) of silica-based colloidal crystals onto hydrophobic and hydrophilic substrates and analyzed how the ink composition and drying morphology affected the printing. Wang et al.[8] used fluorinated patterned silica surfaces to study the effect of dewetting of water-based conducting polymer inks and found that the liquid viscosity and thickness were the controlling factors for the dewetting process. A similar study by Pudas et al.[9] investigated the effect of particulate conductive polymer-based ink lines containing metal particles on paper and plastic substrates. They observed that the substrate smoothness had a superior influence over the line resolution and resistance, which affected the printing quality. Tekin et al.[10] reviewed the effect of ink on substrates, mainly the drying pattern formation and the basic theory behind the droplet formation for piezoelectric print heads. The study highlighted the coffee ring effect, droplet size, and velocity as key parameters affecting the quality of printing (determined using resistivity measurements as a function of curing temperature) on polymer surfaces. Gans et al.[11] investigated perfluorinated substrates using polystyrene polymer printed with nonvolatile acetophenone-based inks to avoid the formation of ring stains during droplet drying, which arises from pinning of the contact edge line convolved with evaporation rate.[12−14] The literature reports that for optimal ink spreading on the substrate, the substrate surface energy should be higher than the ink surface tension.[15] The structure and morphology of the substrate, including its porosity, are also important factors controlling the spreading of ink.[16] Clearly, the wetting of chemically or physically inhomogeneous or patterned substrates is central to this phenomenon. Many studies on these topics describe the physical basis in considerable detail for physically patterned surfaces[17,18] and chemically heterogeneous substrates.[19]

Current technologies for preparing polymeric materials for printing often rely on surface treatment, such as plasma or

Received: March 12, 2019
Revised: April 30, 2019
Published: May 3, 2019

DOI: 10.1021/acs.langmuir.9b00733
Langmuir 2019, 35, 7155−7160

corona discharge, to modify the top polymer layer, remove the dirt, and change the wettability and roughness.[20,21] Strong chemical interactions and surface bonding are facilitated by such surface treatments that induce a high concentration of reactive surface functional groups.[22] These treatments increase the surface free energy and improve the adhesive properties by eliminating pendant bonds from the surface.[23] For optimal adhesion and high-resolution printing, it is important to control the wettability of the polymer surface; to resolve this issue, a wide range of coating technologies have been utilized. Polymer surface modification using organic coatings has been reported extensively using UV-curable polymer coatings,[24] photograft polymers,[25] and initiated chemical vapor deposition.[26] Inorganic coating techniques including plasma-enhanced chemical vapor deposition[27] and magnetron sputtering[26] use an energetic gas phase to deposit inorganic materials onto polymeric substrates. Enhancement of corrosion resistance, hardness, and heat and electric conductivity of polymer surfaces is achieved using metallurgical coatings from chemical electro-less and vapor plating techniques.[28,29] However, these high-energy processes suffer from a lack of scalability or sustainability. Cellulose derivative coatings present an attractive alternative; however, some can absorb ink and swell when printed on, limiting the printing resolution.[22] Recently, Nechyporchuk et al. investigated nanocellulose in the form of cellulose nanocrystals (CNCs), cellulose nanofibrils (CNFs), and carboxymethylated cellulose nanofibrils (CCNFs) for the consolidation of painting canvases.[30] Compared to the native canvas fibers, the nanocellulose coatings had a higher degree of crystallinity and good film-forming properties, facilitating stable and reversible canvas consolidation. The importance of surface roughness was highlighted by Nechyporchuk et al., using cellulose nanofibrils (CNFs) mixed with a plasticizer as a coating on woven cotton fabrics.[31] High-resolution and high-speed printing was enabled by this CNF coating, which facilitated the precise control of ink droplet deposition on the substrate.

Polystyrene, due to its low surface free energy (~43 KJ m^{-2}) and hydrophobicity, is generally a challenging surface for printing and gluing, despite its immense application in thermoformed packaging.[22] In this study, we have developed an effective method to inkjet print water-based ink onto hydrophobic polystyrene using aligned cellulose nanocrystal coatings. The alignment is achieved by utilizing template-assisted self-assembly (TASA) of the CNCs from crack-free wrinkled surfaces. Such soft lithographical surface patterns are prepared via plasma treatment of strained poly(dimethylsiloxane) (PDMS) substrates with a subsequent relaxation that leads to periodic sinusoidal surface corrugations.[32,33] This provides a sustainable printing technology without affecting the properties of the underlying hydrophobic polymer by preventing the spread of ink and achieving a better printing resolution. Further, this technique is readily industrially scalable using roll-to-roll technology.

2. EXPERIMENTAL DETAILS

2.1. Materials. Cellulose nanocrystals (CNCs, 12.2 wt % in water) were purchased from the University of Maine Process Development Center. The sulfur content of the the dried CNCs was determined to be 0.67% using elemental analysis. From the AFM imaging analysis, the CNCs used in this study had average dimensions of 210 ± 26 nm (length) by 5.4 ± 1.1 nm (width). The size polydispersity was found to be 0.342. The surface charge density was determined previously as 14.1 nm^2/charge.[46] Dispersions of 5 mg/mL CNC were used for spin-coating, without further additives. The ionic strength at this dilution was determined as 0.27 mM, and the counterions to the surface sulfate ester moieties are primarily protons. Polystyrene crystals (PS_158K) were purchased from BASF, Germany. For the polystyrene solution, analytical grade toluene was purchased from Merck, Germany. Poly(ethylene oxide) (PEO, average molecular weight ($\underline{M}_V$), 400,000 g mol^{-1}) was used as a release agent for aligned CNC preparation and was purchased from Sigma-Aldrich, USA. Silicone elastomer curing agent and Sylgard 184 silicone elastomer base (Dow Corning Corporation, USA) were used and prepared as per the manufacturer's instructions for polydimethylsiloxane (PDMS). For the printing technique and contact angle measurements, films of polystyrene were prepared by evaporating the polystyrene (5 wt %) toluene solution at room temperature overnight. The ink (water-based dye) for printing on polymer surfaces was purchased from EPSON, Australia (cartridge 29XL, black). The surface tension of this ink has been previously reported[45] as 38.8 mN/m.

2.2. Instrumental Techniques. Atomic force microscopy (AFM, JPK Nanowizard 3) in alternating contact, AC mode was used for the morphological analysis of the substrates. Bruker NCHV tapping mode cantilevers were employed. A spin coater (Laurell Technologies, WS-400BZ-6NPP/LITE) was used to synthesis PEO/CNC coating on wrinkled PDMS. A low-pressure plasma MicroSys apparatus (Roth & Rau, Wüstenbrand, Germany) with a microwave source (~10^{-6} bar) of 800 W with nitrogen gas was used to create wrinkled PDMS. An air plasma chamber (model PDC 002, Harrick Scientific Corporation, USA) with a 30 W plasma power was used to activate the wrinkled PDMS. To measure the wettability of water and ink on different surfaces, a contact angle measuring set-up (Dataphysics OCA35) was used. An inkjet piezoelectric printer (EPSON, XP-245) was used to print the surfaces with text.

2.3. PDMS Wrinkles and Aligned CNC Preparation. The wrinkles were achieved by stretching using a customized stretching device. The strained PDMS was subsequently oxidized to produce crack-free wrinkles upon strain relaxation. The aligned CNC on the polystyrene surface was prepared using a water-mediated transfer process as described in our previous work.[39] The wrinkled PDMS was initially surface-activated using plasma (30 W) for 2 min. The wrinkled PDMS is then spin-coated with 20 μL of PEO (1 wt %) at 2500 rpm 60 s, followed by the CNC (5 mg/mL) deposition using spin-coating at the same conditions used for PEO. The prepared template with CNC was then stamped onto the polystyrene surface with the help of a tiny droplet of water (~2 μL), which facilitates the transfer of aligned CNCs onto the polystyrene surface. The PDMS stamp is carefully peeled-off from the polystyrene surface after 6 h to facilitate appropriate evaporation of water that influences the CNC transfer.

3. RESULTS AND DISCUSSION

3.1. PDMS Wrinkles, Oxidation Time, and CNC Concentration. Crack-free wrinkled templates[34,35] were achieved using a known wrinkling procedure[36−38] (uniaxially stretching, surface oxidizing, and then relaxing) employing elastomeric PDMS as the substrate at different oxidation times (Figure S1). The process of wrinkle formation and the method of preparing aligned CNC coatings on polystyrene are shown schematically in Figure 1(i−vi) with details provided in the Experimental Details section. Well-ordered, crack-free wrinkles were obtained at a strain of 30% and 135 s oxidation time (Figure 1a), resulting in a corrugation wavelength of 850 nm and a corrugation height of 120 nm. We previously showed that the level of ordering from printing aligned CNC was best with a wrinkle periodicity of ~700 nm.[39] Poly(ethylene oxide) (PEO) was applied to the wrinkled PDMS template as a nonadhesive agent to release the CNCs that are then deposited onto the PEO-coated template via spin-coating. To load the

DOI: 10.1021/acs.langmuir.9b00733
Langmuir 2019, 35, 7155−7160

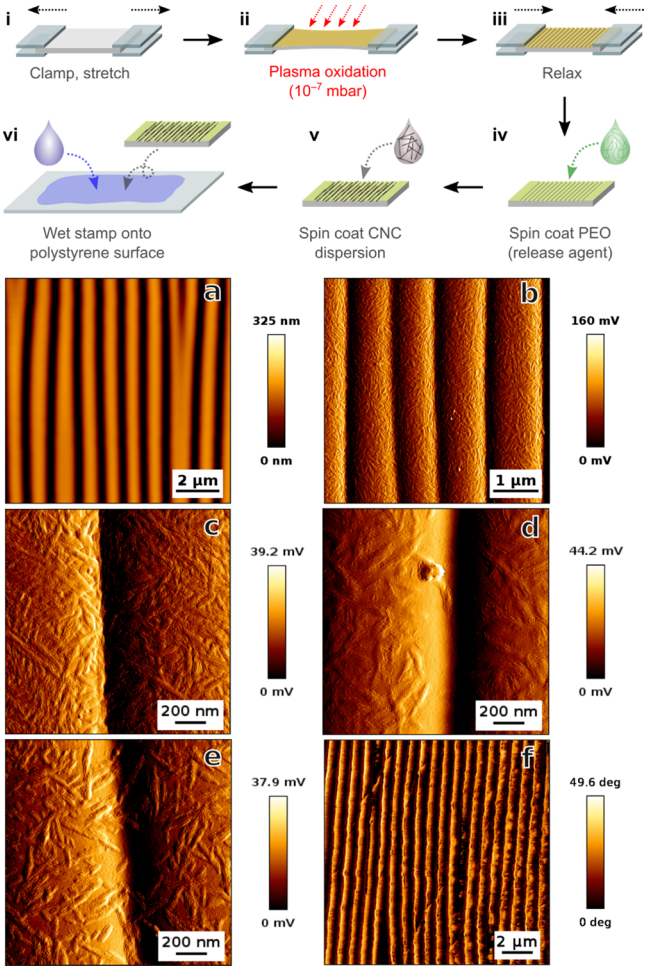

Figure 1. (i–vi) Schematic representation illustrating the preparation of aligned CNC on the polystyrene surface using crack-free wrinkling technology. Topographical atomic force microscopy (AFM) images showing (a) topology of wrinkled PDMS templates (height profile) prepared using 30% strain and 135 s oxidation time; (b) the sample in (a) spin-coated with PEO followed by CNC (5 mg/mL) (amplitude image), both at 2500 rpm; (c) same as (b) but with 3 mg/mL CNC; (d) same as (b) but with 1 mg/mL CNC, and (e) same as (b) but with 0.5 mg/mL CNC. (f) AFM phase image of PDMS stamp after stamping on polystyrene, showing the effectiveness of the CNC transfer.

wrinkled substrate with CNCs, different spin-coating speeds ranging from 2000 to 2500 rpm were tested to determine the effect on the spreading of CNC suspensions; resolution was similar in all cases (Figure S1). Hence, spin-coating at 2500 rpm was used, and the morphology of the CNCs was analyzed using AFM as seen in Figure 1b. To understand the effect of CNC concentration on the degree of CNC alignment on the wrinkled PDMS, concentrations of 3, 1, and 0.5 mg/mL were spin-coated onto crack-free wrinkled PDMS surfaces as shown in Figure 1c–e, respectively, with PEO spin-coating as an initial step. All results were similar, indicating that the CNC concentration is not an important variable. All subsequent CNC aligned surfaces were prepared at a 135 s PDMS oxidation time, 30% PDMS strain, and 5 mg/mL CNC with PEO (1 wt %). The effectiveness of the CNC transfer (Figure 1f) was observed through AFM imaging of the PDMS template after wet stamping. CNC remnants were negligible, indicating the effectiveness of the CNC transfer. The thickness of the transferred CNC pattern features on the polystyrene substrate was obtained from AFM height profiles and was found to be 20 ± 4 nm (see the Supporting Information), indicating that the features indeed comprise multiple stacked CNCs (the features are ~3–5 CNC in thickness with a maximum height on average), explaining the strong pinning of liquid contact lines, discussed in the following sections.

3.2. Polystyrene with CNC, Roughness Analysis, and Contact Angle Measurements. The morphologies of the original polystyrene surface as well as those coated with random CNC and aligned CNC were investigated using AFM as seen in Figure 2a–c. The hole-like perforations of the original (nonplasma-treated) polystyrene film evolve during drying as the solvent (toluene) evaporates. To detect whether plasma treatment affected the surface morphology of polystyrene, AFM was performed after the plasma exposure (Figure S2); analysis showed a roughness of 2.1 ± 1.2 nm,

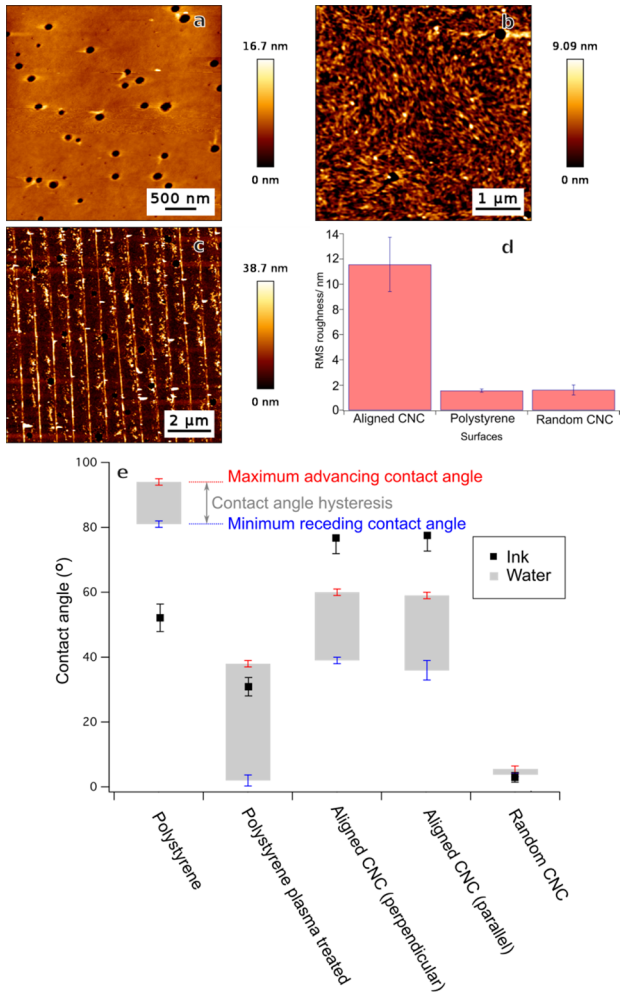

Figure 2. Atomic force microscopy (AFM) images showing the topology of (a) polystyrene (nonplasma-treated); (b) random CNC on plasma-treated polystyrene; and (c) Aligned CNC on plasma-treated polystyrene. (d) Column graph comparing the roughness of the surfaces in (a–c); (e) Maximum advancing and minimum receding contact angles of water and the equilibrium contact angle of ink on the model surfaces in this study: as-prepared polystyrene, plasma-treated polystyrene, aligned CNC on polystyrene (where the contact angle is measured separately perpendicular and parallel to the axis of alignment), and random CNC on polystyrene.

DOI: 10.1021/acs.langmuir.9b00733
Langmuir 2019, 35, 7155–7160

similar to polystyrene without plasma treatment. This confirms that the plasma treatment changed the surface chemistry but not the roughness. It is widely accepted that the surface wettability is strongly influenced by the roughness of the surface, with asperities and heterogeneities inducing different levels of pinning.[40,41] Hence, the roughness was calculated from the AFM height images. Comparison of the surfaces in Figure 2d indicates that the aligned CNC has a high degree of (in this case, ordered) roughness compared to other surfaces, owing to its induced surface structure.

To determine the effect of aligned CNC coatings on the surface wettability of polystyrene, contact angle measurements were carried out. The maximum advancing and minimum receding contact angles of water (as a model for water-based inks) as well as the equilibrium contact angle of a commercial inkjet ink on all surfaces were measured (Figure 2e). The difference between the maximum advancing contact angle and the minimum receding contact angle defines the contact angle hysteresis (CAH).[42]

The aligned CNC on the plasma-treated polystyrene showed higher contact angle values compared to random CNC on plasma-treated polystyrene and plasma-treated polystyrene with no CNC present. The contact angles were similar, both perpendicular and parallel to the alignment axis of the aligned CNC surface, supporting observations from our previous work.[39] Mild plasma treatment of the polystyrene surface is required to facilitate effective transfer of the CNCs; we favored plasma over an additional coating with a cationic polyelectrolyte to facilitate transfer, as this treatment produces more robust coatings. The alignment technique was found to increase the surface roughness (owing to surface patterning), yielding higher contact angles with water and inducing strong pinning effects, as expected from previous work.[39] Randomly oriented CNCs on plasma-treated polystyrene render a surface that is highly hydrophilic in nature, owing to the inherent hydrophilicity of the CNCs. This also provides context as to the choice for CNC as a patterning material. Polymers with similar chemistry such as carboxymethylcellulose would not be patterned by the template and so would provide a homogeneous hydrophilic coating.

A similar trend was observed with contact angle measurements of ink on the surfaces examined. The wettability of water-based ink was considerably lower on the aligned CNC (both parallel and perpendicular to alignment), again, owing to pinning effects.[40] We therefore anticipated that this pinning would lead to an effective printing by retaining the ink droplet boundaries in place. This would maintain the ink droplets at their deposition site, preventing bleeding and feathering effects caused by wettable surfaces or movement across the surface after the droplet impact as is typically seen for hydrophobic surfaces.

3.3. Ink Printing on Polystyrene Coated with Aligned CNC. The hypothesis that aligned CNC coatings on polystyrene improve printing resolution was tested by inkjet printing of a black ink using a regular piezoelectric printer onto the surfaces of interest. Although the ink has quite a different composition to water (such inks generally contain 20−30% water-miscible organic solvents such as methanol, along with dyes and/or pigments) and a lower surface tension (38.8 mN/m), it is nevertheless a hydrophilic and water-based liquid; thus, we expect broadly the results of our tests above on wettability transpose. The text printed on aligned CNCs stamped onto polystyrene is very clear, whereas the ink bleeds and feathers on both the random CNC coating on polystyrene and the unmodified polystyrene surface as seen in Figure 3a−c.

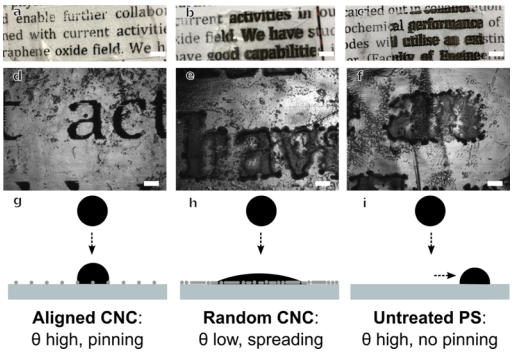

Figure 3. Photographs of text printed onto test surfaces and corresponding optical microscopy images for (a, d) aligned CNC on polystyrene, (b, e) random CNC spin-coated onto polystyrene, and (c, f) polystyrene surface. The white scale bars in (a−c) correspond to 700 μm, whereas in (d−f), they correspond to 200 μm. (g−i) Schematic representation of the ink behavior on aligned CNC, random CNC, and untreated polystyrene surface with varying pinning effects.

Optical microscopy reveals the letter "a" to be printed very clearly without bleeding or feathering of the ink, while the same letter "a" is unclear on both random CNC on polystyrene and polystyrene surfaces (Figure 3d− f). Ink spreading was observed on the polystyrene and the random CNC-coated polystyrene surfaces. A schematic representation of the assumed behavior of ink droplets on different surfaces with varied pinning effects is shown in Figure 3(g−i). This indicates that the ink spread is influenced by surface structuring using alignment, inducing pinning effects[43] with commensurate high surface roughness, thus preventing any contact line motion of the printed droplets. The unmodified polystyrene has a high contact angle with water/ink due to its hydrophobic surface; without the hydrophilic pinning sites, droplets would chaotically roll and spread on the surface, reducing printing resolution by creating bleeding and feather marks.[44] The periodic wavelength of the aligned CNC (~850 nm) is far less than the impacted droplet diameter (typically in the 10−20 μm range), meaning that the ink droplet boundaries pin on multiple cellulose features.[45] Surface engineering polystyrene using aligned CNC coatings thus helps to achieve the highest printing resolution. In terms of scale, it should be noted that piezoelectric inkjet printing heads produce droplets typically in the 10−100 μm range. These result in dot sizes when impacted/spread on the printing surface of around 40−200 μm. Thus, each droplet interacts with many CNC features on the surface (rather than bridging across just a few) and samples the average wettability of the overall surface texture (rather than the granularity of pinning at only a few CNC features).

3.4. Quantitative Analysis of Ink Spreading. The enhancement of the printing resolution using aligned CNC was quantified by calculating the spreading factor of the letter **a** printed on a normal paper as compared to uncoated polystyrene and polystyrene coated with aligned CNC or random CNC (Figure 4). The spreading factor was calculated by measuring the width of the lines making up the character at various positions and calculating the average ratio of the line thickness between the test surfaces and the character printed

DOI: 10.1021/acs.langmuir.9b00733
Langmuir 2019, 35, 7155−7160

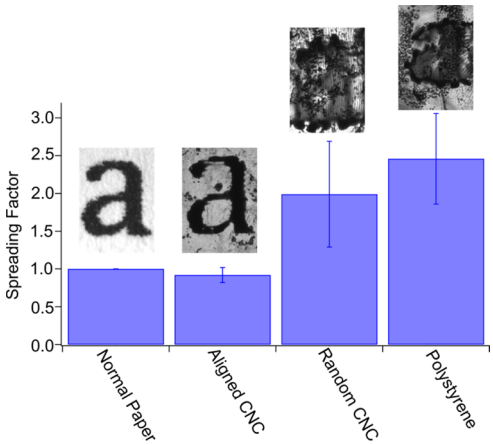

Figure 4. Column graph showing the calculated spreading factor of ink on a normal (80 gsm white) paper as compared to coated surfaces: aligned CNC on polystyrene, random CNC on polystyrene, and uncoated polystyrene, along with optical images of the letter "a" printed on each surface.

on a regular 80 gsm white paper. The spreading factor is almost identical to the paper in the case of the aligned CNC-coated surface. Higher spreading factors for both random CNC-coated polystyrene and uncoated polystyrene surfaces provide a quantitative measurement of the ink spreading, indicating ~2× loss of resolution in each case compared to the aligned CNC.

4. CONCLUSIONS

In summary, highly ordered wrinkled PDMS templates with a wavelength of ~850 nm was used to transfer aligned cellulose nanocrystal coatings onto polystyrene films, used as a model hydrophobic polymer surface. The alignment of cellulose nanocrystals locally increased the roughness of the surface in an ordered fashion, providing sites for liquid interface pinning and hence decreasing the wettability in a controlled manner. Such aligned cellulose nanocrystal-coated polystyrene surfaces prevent ink bleeding in inkjet printing applications, typically using water-based ink, thus enhancing the printing resolution. Further research could be carried out with a range of other hydrophobic surfaces, where printing resolution is a limiting factor due to the ink bleeding. It would also be interesting to explore other hydrophilic particles such as clay platelets or silica spheres as patterning materials for such surfaces. However, the appeal of CNCs remains in terms of their sustainable nature, suitable surface chemistry, and shape anisotropy that favors strong adhesion with the substrate. The current study may serve as a roadmap for investigating the printing of functional ink or biological fluids for high-throughput testing applications. In scaling this process to application, spin-coating would become impractical and so the other methods such as dip- and spray-coating of the CNC dispersion onto the template should be explored. Furthermore, robustness of such coatings would be crucial in their application, and so abrasion and scratch testing could be undertaken to explore this.

■ ASSOCIATED CONTENT

Supporting Information

The Supporting Information is available free of charge on the ACS Publications website at DOI: 10.1021/acs.langmuir.9b00733.

Optimization of PDMS wrinkles at different oxidation times and spin-coating conditions, AFM image of polystyrene surface after 2 min of plasma exposure, and AFM height image of printed CNC on polystyrene surface and the corresponding height profile (PDF)

■ AUTHOR INFORMATION

Corresponding Author

*E-mail: rico.tabor@monash.edu. Tel.: +61 3 9905 4558.

ORCID

Andreas Fery: 0000-0001-6692-3762
Gil Garnier: 0000-0003-3512-0056
Rico F. Tabor: 0000-0003-2926-0095

Funding

This work was supported in part by the award of an ARC Future Fellowship to R.F.T.

Notes

The authors declare no competing financial interest.

■ ACKNOWLEDGMENTS

The State Government of Victoria and the Monash Centre for Atomically Thin Materials are acknowledged for the award of Victoria India Doctoral Scholarship and top-up scholarship, respectively (R.P.). The financial support by the German Academic Exchange Service (DAAD)—Thematic Network *Melbourne−Bayreuth Polymer/Colloid Network* e Federal Ministry of Education and Research (BMBF) is acknowledged. Thanks to M. Nitschke for the assistance with the plasma treatment and sample preparation.

■ ABBREVIATIONS

CNCstabcellulose nanocrystals
PEOtabpoly(ethylene oxide)
PDMStabpoly(dimethylsiloxane)
AFMtabatomic force microscopy
PStabpolystyrene

■ REFERENCES

(1) de Gans, B.-J.; Duineveld, P. C.; Schubert, U. S. Inkjet Printing of Polymers: State of the Art and Future Developments. *Adv. Mater.* **2004**, *16*, 203−213.

(2) Sirringhaus, H.; Kawase, T.; Friend, R. H.; Shimoda, T.; Inbasekaran, M.; Wu, W.; Woo, E. P. High-Resolution Inkjet Printing of All-Polymer Transistor Circuits. *Science* **2000**, *290*, 2123−2126.

(3) Shimoda, T.; Morii, K.; Seki, S.; Kiguchi, H. Inkjet Printing of Light-Emitting Polymer Displays. *MRS Bull.* **2003**, *28*, 821−827.

(4) Katstra, W. E.; Palazzolo, R. D.; Rowe, C. W.; Giritlioglu, B.; Teung, P.; Cima, M. J. Oral Dosage forms Fabricated by Three Dimensional Printing. *J. Controlled Release* **2000**, *66*, 1−9.

(5) Garnier, F.; Hajlaoui, R.; Yassar, A.; Srivastava, P. All-Polymer Field-Effect Transistor Realized by Printing Techniques. *Science* **1994**, *265*, 1684−1686.

(6) Grace, J. M.; Botticelli, V.; Freeman, D. R.; Kosel, W.; Spahn, R. G. Salt Bath Test for assessing the Adhesion of Silver to Poly(ethylene terephthalate) web. *J. Adhes. Sci. Technol.* **1993**, *7*, 885−896.

DOI: 10.1021/acs.langmuir.9b00733
Langmuir 2019, 35, 7155−7160

(7) Park, J.; Moon, J. Control of Colloidal Particle Deposit Patterns within Picoliter Droplets Ejected by Ink-Jet Printing. *Langmuir* **2006**, *22*, 3506−3513.
(8) Wang, J. Z.; Zheng, Z. H.; Li, H. W.; Huck, W. T. S.; Sirringhaus, H. Dewetting of Conducting Polymer Inkjet Droplets on Patterned Surfaces. *Nat. Mater.* **2004**, *3*, 171.
(9) Pudas, M.; Halonen, N.; Granat, P.; Vähäkangas, J. Gravure Printing of Conductive Particulate Polymer Inks on Flexible Substrates. *Prog. Org. Coat.* **2005**, *54*, 310−316.
(10) Tekin, E.; Smith, P. J.; Schubert, U. S. Inkjet Printing as a Deposition and Patterning Tool for Polymers and Inorganic Particles. *Soft Matter* **2008**, *4*, 703−713.
(11) de Gans, B.-J.; Schubert, U. S. Inkjet Printing of Well-Defined Polymer Dots and Arrays. *Langmuir* **2004**, *20*, 7789−7793.
(12) Deegan, R. D.; Bakajin, O.; Dupont, T. F.; Huber, G.; Nagel, S. R.; Witten, T. A. Capillary Flow as the Cause of Ring Stains from Dried Liquid Drops. *Nature* **1997**, *389*, 827.
(13) Deegan, R. D.; Bakajin, O.; Dupont, T. F.; Huber, G.; Nagel, S. R.; Witten, T. A. Contact Line Deposits in an Evaporating Drop. *Phys. Rev. E* **2000**, *62*, 756−765.
(14) Deegan, R. D. Pattern Formation in Drying Drops. *Phys. Rev. E* **2000**, *61*, 475−485.
(15) Pesach, D.; Marmur, A. Marangoni Effects in the Spreading of Liquid Mixtures on a Solid. *Langmuir* **1987**, *3*, 519−524.
(16) Holman, R. K.; Uhland, S. A.; Cima, M. J.; Sachs, E. Surface Adsorption Effects in the Inkjet Printing of an Aqueous Polymer Solution on a Porous Oxide Ceramic Substrate. *J. Colloid Interface Sci.* **2002**, *247*, 266−274.
(17) Seemann, R.; Brinkmann, M.; Kramer, E. J.; Lange, F. F.; Lipowsky, R. Wetting Morphologies at Microstructured Surfaces. *Proc. Nat. Acad. Sci.* **2005**, *102*, 1848−1852.
(18) Nosonovsky, M.; Bhushan, B. Patterned Nonadhesive Surfaces: Superhydrophobicity and Wetting Regime Transitions. *Langmuir* **2008**, *24*, 1525−1533.
(19) Extrand, C. W. Contact Angles and Hysteresis on Surfaces with Chemically Heterogeneous Islands. *Langmuir* **2003**, *19*, 3793−3796.
(20) Tuominen, M.; Lahti, J.; Lavonen, J.; Penttinen, T.; Räsänen, J. P.; Kuusipalo, J. The Influence of Flame, Corona and Atmospheric Plasma Treatments on Surface Properties and Digital Print Quality of Extrusion Coated Paper. *J. Adhes. Sci. Technol.* **2010**, *24*, 471−492.
(21) Gooch, J. W. Polyimide. In *Encyclopedic Dictionary of Polymers*; Gooch, J. W., Ed.; Springer: New York, NY, 2011; 562−562.
(22) Izdebska, J.; Thomas, S. *Printing on Polymers: Fundamentals and Applications*; Elsevier: USA, 2016.
(23) Kusano, Y. Atmospheric Pressure Plasma Processing for Polymer Adhesion: A Review. *J. Adhes.* **2014**, *90*, 755−777.
(24) Erbay, B. T.; Serhatlı, I. E. Synthesis of Bis[(4-hydroxyethoxy)-phenyl]Sulfone containing Urethane Acrylates and their Applications. *Prog. Org. Coat.* **2013**, *76*, 1−10.
(25) Ma, H.; Davis, R. H.; Bowman, C. N. A Novel Sequential Photoinduced Living Graft Polymerization. *Macromolecules* **2000**, *33*, 331−335.
(26) Lau, K. K. S.; Gleason, K. K. Initiated Chemical Vapor Deposition (iCVD) of Poly(alkyl acrylates): An Experimental Study. *Macromolecules* **2006**, *39*, 3688−3694.
(27) Alexandrov, S. E.; Hitchman, M. L. Chemical Vapor Deposition Enhanced by Atmospheric Pressure Non-thermal Non-equilibrium Plasmas. *Chem. Vap. Deposition* **2005**, *11*, 457−468.
(28) Liao, Y.; Cao, B.; Wang, W.-C.; Zhang, L.; Wu, D.; Jin, R. A Facile Method for Preparing Highly Conductive and Reflective Surface-Silvered Polyimide Films. *Appl. Surf. Sci.* **2009**, *255*, 8207−8212.
(29) Schulz, U.; Kaiser, N. Vacuum Coating of Plastic Optics. *Prog. Surf. Sci.* **2006**, *81*, 387−401.
(30) Nechyporchuk, O.; Kolman, K.; Bridarolli, A.; Odlyha, M.; Bozec, L.; Oriola, M.; Campo-Francés, G.; Persson, M.; Holmberg, K.; Bordes, R. On the Potential of Using Nanocellulose for Consolidation of Painting Canvases. *Carbohydr. Polym.* **2018**, *194*, 161−169.
(31) Nechyporchuk, O.; Yu, J.; Nierstrasz, V. A.; Bordes, R. Cellulose Nanofibril-Based Coatings of Woven Cotton Fabrics for Improved Inkjet Printing with a Potential in E-Textile Manufacturing. *ACS Sustainable Chem. Eng.* **2017**, *5*, 4793−4801.
(32) Béfahy, S.; Lipnik, P.; Pardoen, T.; Nascimento, C.; Patris, B.; Bertrand, P.; Yunus, S. Thickness and Elastic Modulus of Plasma Treated PDMS Silica-like Surface Layer. *Langmuir* **2010**, *26*, 3372−3375.
(33) Rhee, D.; Lee, W. K.; Odom, T. W. Crack-Free, Soft Wrinkles Enable Switchable Anisotropic Wetting. *Angew. Chem., Int. Ed.* **2017**, *56*, 6523−6527.
(34) Tebbe, M.; Mayer, M.; Glatz, B. A.; Hanske, C.; Probst, P. T.; Müller, M. B.; Karg, M.; Chanana, M.; König, T. A. F.; Kuttner, C.; Fery, A. Optically Anisotropic Substrates via Wrinkle-Assisted Convective Assembly of Gold Nanorods on Macroscopic Areas. *Faraday Discuss.* **2015**, *181*, 243−260.
(35) Glatz, B. A.; Fery, A. The influence of plasma treatment on the elasticity of the in situ oxidized gradient layer in PDMS: towards crack-free wrinkling. *Soft Matter* **2019**, *15*, 65−72.
(36) Lu, C.; Möhwald, H.; Fery, A. A Lithography-Free Method for Directed Colloidal Crystal Assembly Based on Wrinkling. *Soft Matter* **2007**, *3*, 1530−1536.
(37) Glatz, B. A.; Tebbe, M.; Kaoui, B.; Aichele, R.; Kuttner, C.; Schedl, A. E.; Schmidt, H.-W.; Zimmermann, W.; Fery, A. Hierarchical Line-Defect Patterns in Wrinkled Surfaces. *Soft Matter* **2015**, *11*, 3332−3339.
(38) Schweikart, A.; Fery, A. Controlled wrinkling as a novel method for the fabrication of patterned surfaces. *Microchim. Acta* **2009**, *165*, 249−263.
(39) Prathapan, R.; Berry, J. D.; Fery, A.; Garnier, G.; Tabor, R. F. Decreasing the Wettability of Cellulose Nanocrystal Surfaces Using Wrinkle-Based Alignment. *ACS Appl. Mater. Interfaces* **2017**, *9*, 15202−15211.
(40) Kurogi, K.; Yan, H.; Tsujii, K. Importance of Pinning Effect of Wetting in Super Water-Repellent Surfaces. *Colloids Surf., A* **2008**, *317*, 592−597.
(41) Ramos, S. M. M.; Charlaix, E.; Benyagoub, A. Contact Angle Hysteresis on Nano-Structured Surfaces. *Surf. Sci.* **2003**, *540*, 355−362.
(42) Extrand, C. W.; Kumagai, Y. An Experimental Study of Contact Angle Hysteresis. *J. Colloid Interface Sci.* **1997**, *191*, 378−383.
(43) Lee, Y.; Park, S.-H.; Kim, K.-B.; Lee, J.-K. Fabrication of Hierarchical Structures on a Polymer Surface to Mimic Natural Superhydrophobic Surfaces. *Adv. Mater.* **2007**, *19*, 2330−2335.
(44) Burachinsky, B. V.; Jacob, Y. P. Printing on Polystyrene. US3397074A,1968.
(45) Khan, M. S.; Fon, D.; Li, X.; Tian, J.; Forsythe, J.; Garnier, G.; Shen, W. Biosurface Engineering through Ink Jet Printing. *Colloids Surf., B* **2010**, *75*, 441−447.
(46) Prathapan, R.; Thapa, R.; Garnier, G.; Tabor, R. F. Modulating the Zeta Potential of Cellulose Nanocrystals using Salts and Surfactants. *Colloids Surf., A* **2016**, *509*, 11−18.

DOI: 10.1021/acs.langmuir.9b00733
Langmuir 2019, 35, 7155−7160